

# Static wetting of a liquid drop on a solid

GE WANG, J. J. LANNUTTI

*Department of Materials Science and Engineering, The Ohio State University, Columbus, OH 43210, USA*

---

A variational treatment of sessile drop shape is provided. The surface energy and the driving force for drop spreading are also analysed. This analysis demonstrates that the Young equation does indeed give the equilibrium contact angle in a gravity-free environment.

---

## 1. Introduction

The wetting and spreading of liquids on solid surfaces is a key phenomenon in brazing and soldering and also in other joining processes such as adhesive bonding. It is also critical in the fabrication of composite materials. For these reasons wetting of solids by liquids has been extensively studied [1].

While the field of wetting and spreading of liquid metals on solid metals has been relatively mature for several decades, significant activity has occurred in the past decade concerning the brazing of ceramics [2] and the interactions between a liquid metal and a non-metallic solid (e.g. ceramics, intermetallics, or composites). The covalent and ionic nature of bonding in ceramics leads to solid surface energies that are usually much lower than those of metals. Consequently, conventional brazing and soldering alloys do not wet ceramics and glasses.

In “active metal” brazing a small quantity of a reactive metal such as Ti, Zr, Hf or V is added to a conventional brazing alloy. During brazing some of the reactive metal produces a thin surface layer on the ceramic (or composite). The free energy released by this exothermic reaction provides the driving force for wetting and spreading of the liquid on the ceramic. Although active metal brazing has been widely used, the state-of-the-art does not offer a sufficiently complete understanding of the phenomena to allow accurate theoretical predictions by the end user or the researcher. This forces the manufacturing engineer and the researcher to conduct a large number of experiments to develop a knowledge base sufficient to allow implementation of the process.

As our investigation proceeded we generated additional information concerning wetting and spreading in non-reactive systems including a re-evaluation of the classical Young–Dupre equation and the Bashforth and Adams treatment. Historical development of the understanding of static wetting can be traced back to 1712 when Taylor measured the capillary rise of water between two glass plates [3]. Almost a century later, Young [4] presented his famous relation connecting surface tension and static contact angle. In 1883, Bashforth and Adams [5] published their work on the static shape of a sessile drop. Extensive reviews on static

wetting have since been published by de Gennes [6], Naidich [1], Bikerman [7], and Johnson and Dettre [8].

Wettability of a liquid phase on a solid phase is defined by the contact angle between the liquid drop and a solid surface. “Non-wetting” occurs if an obtuse angle is obtained. “Partial wetting” refers to situations where finite acute contact angles are obtained, while “complete wetting” refers to a zero contact angle.

At the static condition, the contact angle is a direct result of interfacial force balance at the location where three phases meet (i.e. the “contact line”). In the 1950s the validity of the Young equation was challenged by Bikerman [7] because the derivation of the Young equation by a force balance did not consider the vertical component of the liquid surface tension. The most recent derivations of this equation for a sessile drop resulted from minimizing the total free energy of the system [9, 10].

## 2. The shape of a sessile drop

The shape of a sessile drop was examined by Bashforth and Adams [5] in 1883. By analysing the pressure balance inside a sessile drop using the Laplace equation, they determined that a second order differential equation describes the shape of the sessile drop. However, in a gravity field this equation is solved numerically, and the solution requires a knowledge of the curvature of the drop at its summit. Robertson and Lehman [11] proposed a direct energy method to solve for the shape of a sessile drop by numerical integration. However, this treatment requires a knowledge of the height and the base width of the drop. Further mathematical and computational development can be found in texts by Hartland and Hartley [12] and Finn [3].

## 3. Variational treatment of a sessile drop

In previous treatments of sessile drop shape, the boundary conditions were not explicitly stated. A general belief is that the Young equation must be such a condition. The variational method is a powerful tool used to analyse these kinds of static or dynamic systems without requiring a detailed force

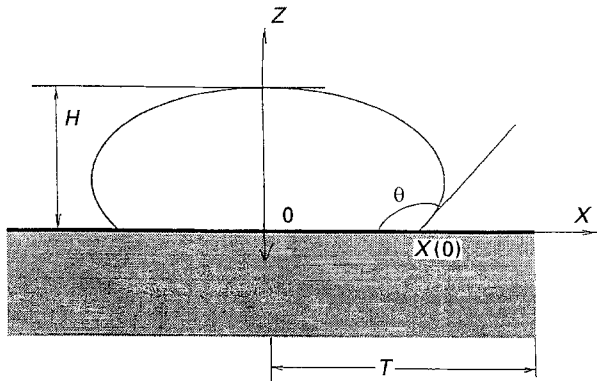


Figure 1 The coordinate system for a sessile drop assumed in the analysis.

analysis. By minimizing the total energy or the entropy production of the system, the governing equations and the "natural" boundary conditions can be derived [13].

A sessile drop and the associated geometric definitions important in the analysis are shown in Fig. 1. Here  $H$  is the height of the drop,  $\theta$  the contact angle,  $x(0)$  the radius of the drop at its bottom, and  $T$  the radius of the circular solid plate underlying the liquid drop.

The total energy of the system is composed of the surface energies of the solid, the liquid, the interfacial energy between the solid and the liquid, and the gravitational potential energy

$$E_{\text{tot}} = E_0 + \pi x^2(0)\sigma_{\text{ls}} + \pi(T^2 - x^2(0))\sigma_{\text{vs}} + 2\pi\sigma_{\text{lv}} \int_0^H x(1 + x'^2)^{1/2} dz + \rho_1 g \pi \int_0^H x^2 z dz \quad (1)$$

Here the first term on the right-hand side is the internal energy other than surface energy and gravitational potential energy, the second term is the interfacial energy between the drop and the solid, the third the solid surface energy, the fourth the surface energy of the liquid drop, and the last the gravitational potential. The volume of the liquid drop is

$$V = \pi \int_0^H x^2 dz \quad (2)$$

The goal of our use of the variational method is to minimize the total energy within the constant volume constraint. Therefore, the Lagrangian multiplier  $\lambda$  is introduced as part of the goal function ( $G$ ).

$$G = E_{\text{tot}} + \lambda V \quad (3)$$

For a static drop, an arbitrary variation of the goal function  $G$  must equal zero, i.e.

$$\delta G = 0 \quad (4)$$

The variation of the goal function may be caused by the variation of the radius of the drop at the bottom  $\delta x(0)$  or the height of the drop  $\delta H$ . The variational

analysis of Equation 1 results in

$$\begin{aligned} \delta G = & 2\pi(\sigma_{\text{ls}} - \sigma_{\text{vs}})x(0)\delta x(0) \\ & + 2\pi\sigma_{\text{lv}}x(H)(1 + x'^2(H))^{1/2}\delta H \\ & + 2\pi\sigma_{\text{lv}} \int_0^H (1 + x'^2(z))^{1/2} \delta x dz \\ & + 2\pi\sigma_{\text{lv}} \int_0^H x(1 + x'^2)^{-1/2} x' \frac{d}{dz} \delta x dz \\ & + \rho_1 g \pi x^2(H)H\delta H + \rho_1 g \pi \int_0^H 2x\delta x z dz \\ & + \lambda \pi x^2(H)\delta H + \lambda \pi \int_0^H 2x\delta x dz = 0 \quad (5) \end{aligned}$$

where  $x'(0)$  and  $x'(H)$  are the derivatives of  $x$  at  $x = 0$  and  $x = H$ , respectively. The second integral in the above equation can be integrated in part and expanded as follows

$$\begin{aligned} 2\pi\sigma_{\text{lv}} \int_0^H x(1 + x'^2)^{-1/2} x' \frac{d}{dz} \delta x dz = & 2\pi\sigma_{\text{lv}}x(H) \\ & \times (1 + x'^2(H))^{-1/2} x'(H)\delta x(H) \\ & - 2\pi\sigma_{\text{lv}}x(0)(1 + x'^2(0))^{-1/2} x'(0)\delta x(0) \\ & - 2\pi\sigma_{\text{lv}} \int_0^H \frac{d}{dz} [x x'(1 + x'^2)^{-1/2}] \delta x dz \quad (6) \end{aligned}$$

Since  $\delta x(0)$ ,  $\delta H$ , and  $\delta x$  are arbitrary variations, each term in Equations 5 and 6 must be zero. Therefore, the following conditions must be satisfied:

$$1. [\dots]\delta x(0) = 0.$$

$$2\pi x(0)\{\sigma_{\text{ls}} - \sigma_{\text{vs}} - \sigma_{\text{lv}}[1 + x'^2(0)]^{-1/2} x'(0)\} = 0 \quad (7)$$

Since  $x(0) \neq 0$ , and  $\cos \theta = -x'(0)[1 + x'^2(0)]^{-1/2}$ , we have

$$\sigma_{\text{ls}} - \sigma_{\text{vs}} + \sigma_{\text{lv}} \cos \theta = 0 \quad (8)$$

One immediately realizes that this is the Young equation which serves as one of the natural boundary conditions in the analysis.

$$2. [\dots]\delta H = 0.$$

$$\begin{aligned} 2\pi\sigma_{\text{lv}}x(H)[1 + x'^2(H)]^{1/2} + \rho_1 g \pi x^2(H)H \\ + \lambda \pi x^2(H) = 0 \quad (9) \end{aligned}$$

This leads to another natural boundary condition

$$x(H) = 0 \quad (10)$$

$$3. [\dots]\delta x(H) = 0.$$

This also leads to Equation 10.

$$4. [\dots]\delta x = 0.$$

$$2\pi\sigma_{\text{lv}}[1 + x'^2]^{1/2} + 2\pi\rho_1 g x z + 2\pi\lambda x$$

$$- 2\pi\sigma_{\text{lv}} \frac{d}{dz} [x x'(1 + x'^2)^{-1/2}] = 0 \quad (11)$$

This equation leads to a second order differential equation

$$\sigma_{lv} \frac{x''}{[1+x'^2]^{3/2}} - \frac{\sigma_{lv}}{x[1+x'^2]^{1/2}} - g\rho_1 z - \lambda = 0 \quad (12)$$

We can prove that this is equivalent to the Bashforth–Adams type sessile drop equation by applying it to the summit of the sessile drop ( $z = H$ ). Thus, one has

$$-\frac{2\sigma_{lv}}{R(H)} = g\rho_1 H + \lambda \quad (13)$$

where  $R(H)$  is the radius of the curvature at the summit of the drop. This radius was also included in the Bashforth–Adams analysis. If we substitute  $R(H)$  for  $\lambda$  using Equation 13 and invoke the coordinate system of Bashforth and Adams, Equation 12 will be identical to the Bashforth–Adams equation. A further examination of the physical meaning of the Lagrangian multiplier reveals that  $\lambda$  is in fact the internal pressure of the drop at its bottom. This conclusion can be reached by applying Equation (12) at the bottom of the drop where  $z = 0$

$$\lambda = -\sigma_{lv} \left( \frac{1}{R_1(0)} + \frac{1}{R_2(0)} \right) \quad (14)$$

Here  $R_1(0)$  and  $R_2(0)$  are the principal radii of curvature at the contact line of the drop. From the Laplace equation (see e.g. Finn [3]), the physical meaning of  $\lambda$  is indeed the pressure difference between the inside and the outside of the drop at its bottom. If we take the pressure reference point to be inside the bottom of the drop,  $\lambda$  is then the external pressure.

#### 4. Pressure exerted by the drop against its base

The hydrostatic pressure inside the liquid drop depends only on its height. Inside the drop at any given height, the pressure will be the same regardless of its distance from the central axis. This is also true for all points at the bottom of the drop. Therefore the pressure against the base is uniformly distributed and can be calculated by the total force exerted by the weight of the drop divided by the contact area (Fig. 2)

$$p(\text{bottom}) = \frac{\rho_1 g V}{\pi x(0)^2} \quad (15)$$

On the other hand, pressure can also be calculated by the summation of the pressure inside the drop Equations 13 or 14 with reference to the constant external pressure and the pressure due to the surface tension at the contact line. Therefore

$$p(\text{bottom}) = -\lambda - \frac{2\pi x(0)\sigma_{lv} \sin \theta}{\pi x(0)^2} \quad (16)$$

By equating the right hand terms in Equations 15 and 16, and substituting Equations 13 and 14 for  $\lambda$ , we can relate the volume of the drop to measurable

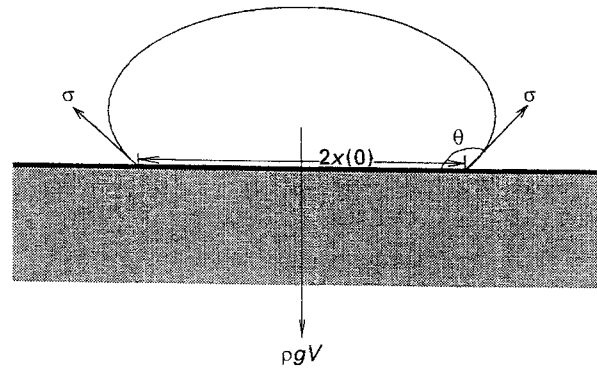


Figure 2 The pressure at the bottom of a sessile drop.

terms

$$V = \frac{\pi x(0)\sigma_{lv}}{\rho_{lg}} \left( \frac{2}{R(H)} - \frac{2 \sin \theta}{x(0)} + \frac{\rho_1 g H}{\sigma_{lv}} \right) \quad (17)$$

$$V = \frac{\pi x(0)\sigma_{lv}}{\rho_{lg}} \left( \frac{1}{R_1(0)} + \frac{1}{R_2(0)} - \frac{2 \sin \theta}{x(0)} \right) \quad (18)$$

Equation 17 is the same as the volume expression obtained by Bashforth and Adams using volume integration.

#### 5. The Young equation

The Young equation (Equation 8) obtained in this analysis appears as one of the natural boundary conditions during the total energy minimization. However, since the virtual displacement  $\delta x(0)$  in the above analysis is not a true independent variable due to the continuity requirement of the entire drop profile (i.e. the variable  $x$  must be equal to  $x(0)$  at  $z = 0$ ), the Young relation thus obtained is not guaranteed to be consistent with the requirement imposed by Equation 12 for the entire drop profile. In the following analysis we will demonstrate that the Young equation is indeed followed by a sessile drop in a gravity-free environment. However in a separate analysis [14] we demonstrate that this equation breaks down in the presence of gravity.

#### 6. Sessile drop in a gravity-free environment

In a gravity-free environment prediction of the shape of a sessile drop is readily solvable. The mathematical equivalence for the gravity-free environment is true not only for  $g = 0$ , but also when the drop has the same density as the gas phase. A fairly good example is a soap bubble with an extremely thin wall. In these situations the third term in Equation 12 is zero.

In a gravity-free environment, the only cause of internal drop pressure is surface curvature. Under equilibrium conditions, the internal pressure is constant regardless of the location. Therefore, the surface curvature of the drop must be the same over the entire surface, and a spherical cap is the only geometrical shape that satisfies this requirement. However, at the base of the drop the pressure cannot be counter-balanced by the curvature, but rather by the tension at

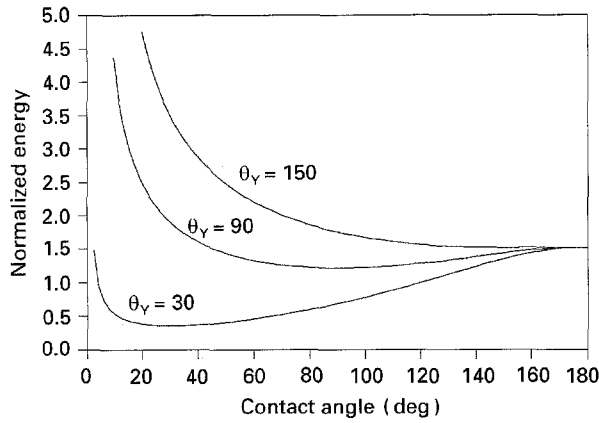


Figure 3 The dependence of the normalized surface energy (Equation 23) on the contact angle under different surface energy combinations which yield Young contact angles of 30, 90 and 150 degrees, respectively.

the contact line. This requirement leads to a physical relationship between the diameter of the base contact area, the contact angle, and the curvature of the spherical cap

$$\frac{2\sigma_{lv}}{R} = \frac{2\pi x(0)\sigma_{lv}\sin\theta}{\pi x(0)^2} \quad (19)$$

Here  $R$  is the radius of the spherical cap,  $\sigma_{lv}$  the surface tension of the liquid drop, and  $x(0)$  the radius of the contact area. The volume of the spherical cap is

$$V = \pi H^2 \left( R - \frac{H}{3} \right) \quad (20)$$

Also, a geometric relationship exists between the height and the radius of the base contact area

$$x(0) = (2RH - H^2)^{1/2} \quad (21)$$

From Equations 19–21 and the Young equation one can solve for  $R$ ,  $x(0)$ ,  $H$  and  $\theta$ . There are four equations for four unknowns and the problem is well defined.

The total surface energy of this system is due to the spherical surface of the drop and the contact area between the drop and the solid base

$$E(\text{surf}) = 2\pi\sigma_{lv}RH + (\sigma_{ls} - \sigma_{sv})\pi x(0)^2 \quad (22)$$

We use these equations to test the Young equation to see if this contact angle gives the minimum system energy in a gravity-free environment. Using Equation 8, Equation 22 can be written as

$$\frac{E(\text{surf})}{\pi\sigma_{lv}V^{2/3}} = \frac{2RH - (2RH - H^2)\cos\Theta_Y}{V^{2/3}} \quad (23)$$

where  $V$  is the volume of the drop and  $\Theta_Y$  is the Young contact angle. The left hand term is a normalized surface energy independent of volume. We define this term as the normalized surface energy (NSE). Fig. 3 shows the NSE as a function of the contact angle (and  $R$  and  $H$  according to Equations 19 and 21) for three different surface and interface energy combinations. These correspond to three different Young contact angles ( $\Theta_Y = 30, 90$  and  $150$  degrees). This figure indeed shows that the Young contact angle

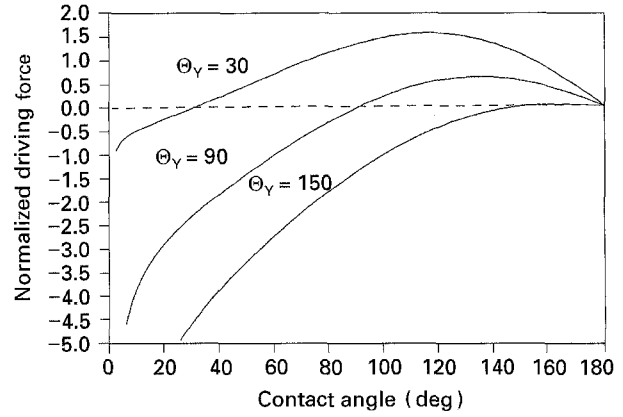


Figure 4 The dependence of the normalized driving force (Equation 24) on the contact angle under different surface energy combinations which yield Young contact angles of 30, 90 and 150 degrees, respectively.

is the equilibrium contact angle, i.e. at the Young contact angle the NSE reaches its minimum. For higher contact angles ( $> 150$  degrees) the energy reduction from the 180 degree configuration to the equilibrium configuration is not very significant. This indicates that greater difficulty is involved in accurately measuring these contact angles.

Fig. 4 demonstrates the thermodynamic driving force acting at the base of the drop as a function of contact angle. This driving force is defined as the negative derivative of the NSE with respect to the normalized radius ( $x(0)/V^{1/3}$ ) of the base contact area. Therefore, this force characterizes the force that acts parallel to the basal plane to push or pull the liquid drop

$$\text{Normalized Driving Force (NDF)} = -\frac{\partial}{\partial x(0)} \left[ \frac{E(\text{surf})}{\pi\sigma_{lv}V^{1/3}} \right] \quad (24)$$

Here the  $1/3$  power of  $V$  reflects the normalization of  $x(0)$  against the cube root of the volume. Again, Fig. 4 shows that this force is zero at the equilibrium contact angle and changes sign at the Young contact angle. This reflects the pulling action exerted on the liquid to spread the drop when the contact angle is smaller than the Young contact angle. A pushing action acts to contract the drop when the contact angle is greater than the Young contact angle. For a contact angle of 180 degrees, no force exists to spread the drop even though the Young contact angle is much smaller than 180 degrees. This indicates that a metastable state exists. Indeed, a local maximal NSE is reached at this point (see Fig. 3). Theoretically speaking, in a gravity-free environment there is no attainable thermodynamic driving force available to spread a spherical liquid drop over a solid plate. A gravity field, or other equivalent accelerating action (vibration, etc.) is necessary to initiate the spreading.

## 7. Effect of surface roughness on static wetting behaviour

If the solid surface is not perfectly smooth, the static contact angle is different from the Young contact

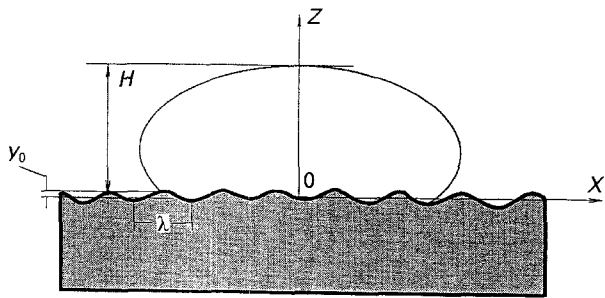


Figure 5 A sessile drop on a hypothetical rough solid surface, where a sine wave surface roughness is assumed, with  $y_0$  as the amplitude and  $\lambda$  as the wave length.

angle predicted by assuming a smooth surface. Wenzel [15] first recognized a “roughness factor,” and noted that the contact angle measured on a rough surface was different from that on a smooth surface. He attributed this difference to the actual surface area on a rough surface being greater than the geometric surface area and defined the ratio between the two surfaces as the roughness factor. Johnson and Dettre [16] later developed a detailed analysis of the roughness effect and related surface roughness to the contact angle hysteresis.

For a rough surface, the contact area between liquid and solid would look like the situation described in Fig. 5. Here the surface roughness is approximated as a sine function with  $y_0$  being the amplitude and  $\lambda$  the wavelength. The liquid–solid contact at the interface exhibits some local detachment and the curvature at point B is less than that at point A. The pressure difference resulting from the curvature difference is then balanced by the vertical component of the liquid surface tension at the local contact line. However, if we assume that the amplitude ( $y_0$ ) is small and ignore both the detailed force balance at the local contact lines and local detachment, Equation 23 can be rewritten as

$$\frac{E(\text{surf})}{\pi\sigma_{lv}V^{2/3}} = \frac{2RH - A\cos\Theta_Y/\pi}{V^{2/3}} \quad (25)$$

where

$$A = \int_0^{x(0)} 2\pi x \left[ 1 + \left( \frac{2\pi y_0}{\lambda} \right)^2 \sin^2 \left( \frac{2\pi x}{\lambda} \right) \right]^{1/2} dx \quad (26)$$

is the contact area between the solid and liquid. Here the assumption is that the sinusoidally-shaped surface roughness has a circular symmetry about the centre of the liquid drop. Fig. 6 shows a calculation of the effect of the surface roughness on the static wetting for  $\Theta_Y = 150$ . A parameter  $\Psi$  is used in the calculation, which is the ratio of the amplitude ( $y_0$ ) and the wavelength ( $\lambda$ ) of the roughness. We see that for high  $\Psi$  values, the static contact angle corresponding to the minimum system energy shifts toward higher angles. This agrees with the observations of Hitchcock *et al.* [17], who found that for most systems the static contact angle increases with increasing roughness parameter ( $R_a/\lambda_a$ ) where  $R_a$  is the amplitude and  $\lambda_a$  the

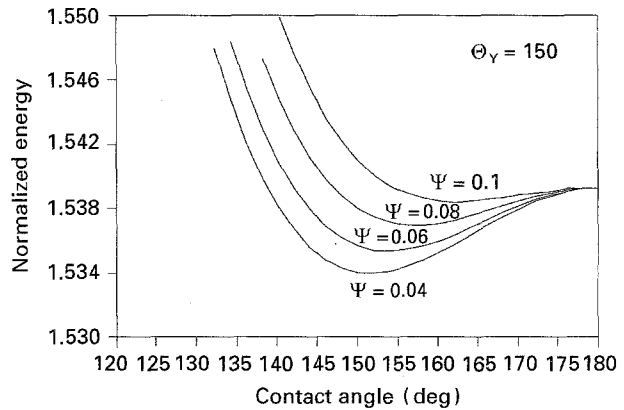


Figure 6 The dependence of the normalized surface energy (Equation 24) on the contact angle using different surface roughness  $\Psi$ . The Young contact angle is assumed to be 150 degrees.

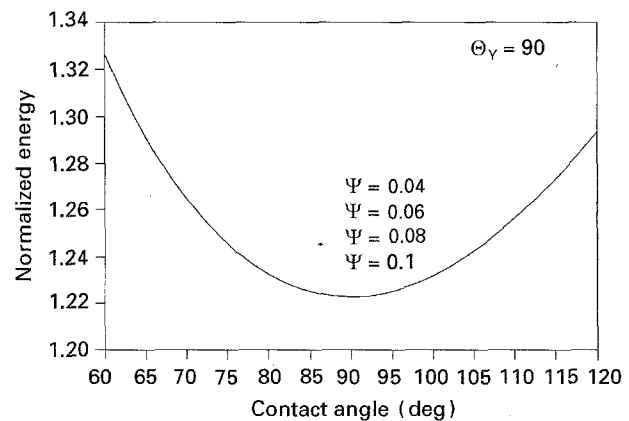


Figure 7 The dependence of the normalized surface energy (Equation 24) on the contact angle using different surface roughness  $\Psi$ . The Young contact angle is assumed to be 90 degrees.

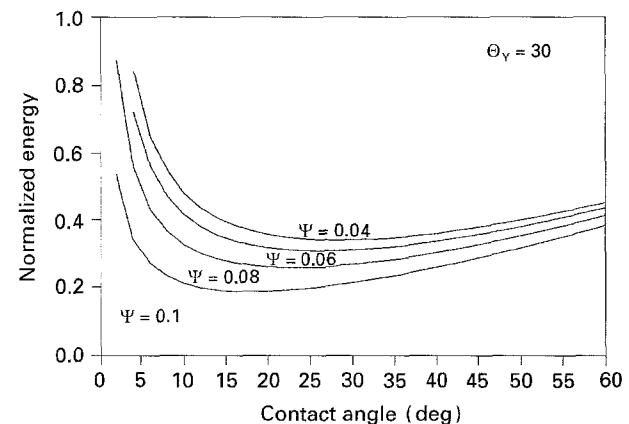


Figure 8 The dependence of the normalized surface energy Equation (24) on the contact angle using different surface roughness  $\Psi$ . The Young contact angle is assumed to be 30 degrees.

wavelength in their nomenclature. The physical meaning for this is that the effective surface area increases as the roughness increases, which can be realized from Equation 25. From Equation 25 the effective surface area modulates the  $\cos\Theta_Y$  term, which in turn results in a shift of the static contact angle. Since  $\cos\Theta_Y$  changes sign at  $\Theta_Y = 90$ , the surface roughness will not change the wetting characteristics (Fig. 7) but will enhance them (Fig. 8).

In other words, a system showing good wetting on a smooth surface will wet better on a rough surface of that same solid. Conversely a system showing poor wetting on a smooth surface will be even more constricted by a rough surface. This explains for example why morning dew forms a better sphere on a hair-covered leaf than on a smooth one.

## 8. Conclusions

1. A variational treatment on the equilibrium shape of a sessile drop is provided.
2. The Young equation appears as one of the "natural" boundary conditions for the minimization of system internal energy.
3. The spreading of a sessile drop in a gravity-free environment is fully analysed as a function of shape, energy, and driving force.
4. The analysis demonstrates that the Young contact angle is indeed the equilibrium contact angle in a gravity-free environment. Here the system energy reaches a minimum and the driving force is zero.
5. At a metastable point (a contact angle of 180 degrees) the energy reaches a local maximum, and the driving force is also zero.
6. Surface roughness does not change the wetting characteristics of a system but instead enhances them.

## References

1. J. V. NAIDICH, *Prog. Surf. Membr. Sci.* **14** (1981) 353.
2. E. S. PARK, J. J. LANNUTTI and J. D. CAWLEY, *J. Am. Ceram. Soc.* **78** (1995) 15
3. R. FINN, "Equilibrium capillary surfaces" (Springer-Verlag, New York, 1986).
4. T. YOUNG, *Phil. Trans. R. Soc. Lond.* **95** (1805) 65.
5. F. BASHFORTH and J. C. ADAMS, "An attempt to test the theories of capillarity action" (Cambridge University Press, London, 1883).
6. P. G. DE GENNES, *Rev. Mod. Phys.* **57** (1985) 827.
7. J. J. BIKERMAN, "Physical surfaces" (Academic Press, New York, 1970) p. 239.
8. R. E. JOHNSON, JR and R. H. DETTRE, *Advan. Chem.* **43** (1964) 112.
9. R. E. JOHNSON, JR, *J. Phys. Chem.* **63** (1959) 1655.
10. J. E. McNUTT and G. M. ANDES, *ibid.* **30** (1959) 1300.
11. W. M. ROBERTSON and G. W. LEHMAN, *J. Appl. Phys.* **39** (1968) 1994.
12. S. HARTLAND and R. W. HARTLEY, "Axisymmetric fluid-liquid interfaces" (Elsevier, New York, 1976).
13. R. S. SCHECHTER, "The variational method in engineering" (McGraw-Hill Book Company, New York, 1967).
14. G. WANG, J. J. LANNUTTI and R. KAPOOR, "Equilibrium contact angle of a sessile drop in a gravity field" (1995), in press.
15. R. N. WENZEL, *Ind. Eng. Chem.* **28** (1936) 988.
16. R. E. JOHNSON, JR and R. H. DETTRE "Surface and colloid science", Volume 2, edited by E. Matijevic (Wiley-Interscience, New York, 1969) p. 85.
17. S. J. HITCHCOCK, N. T. CARROLL and M. G. NICHOLAS, *J. Mater. Sci.* **16** (1981) 714.

Received 19 April  
and accepted 10 October 1994